THE JOURNAL OF PHYSICAL CHEMISTRY Letters

pubs.acs.org/JPCL Letter

Friction Anisotropy of MoS_2: Effect of Tip–Sample Contact Quality

Mohammad R. Vazirisereshk,[#] Kathryn Hasz,[#] Robert W. Carpick,[*] and Ashlie Martini[*]

Cite This: *J. Phys. Chem. Lett.* 2020, 11, 6900–6906 Read Online

ACCESS | Metrics & More | Article Recommendations | Supporting Information

ABSTRACT: Atomic-scale friction measured for a single asperity sliding on 2D materials depend on the direction of scanning relative to the material's crystal lattice. Here, nanoscale friction anisotropy of wrinkle-free bulk and monolayer MoS_2 is characterized using atomic force microscopy and molecular dynamics simulations. Both techniques show 180° periodicity (2-fold symmetry) of atomic-lattice stick–slip friction vs. the tip's scanning direction with respect to the MoS_2 surface. The 60° periodicity (6-fold symmetry) expected from the MoS_2 surface's symmetry is only recovered in simulations where the sample is rotated, as opposed to the scanning direction changed. All observations are explained by the potential energy landscape of the tip–sample contact, in contrast with nanoscale topographic wrinkles that have been proposed previously as the source of anisotropy. These results demonstrate the importance of the tip–sample contact quality in determining the potential energy landscape and, in turn, friction at the nanoscale.

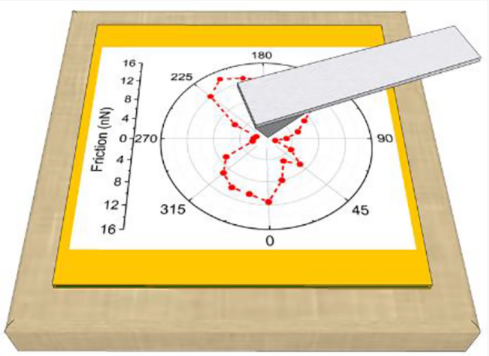

Most physical and mechanical properties of crystalline materials, including friction, are anisotropic to some degree due to the inherent crystallographic symmetry of the materials.[1−4] Friction anisotropy specifically refers to the dependence of friction on the lateral sliding direction or on the relative crystallographic orientation between two sliding surfaces.[5] One of the earliest investigations of friction anisotropy was performed by Hirano et al.[6] in the early 1990s using a surface force apparatus to measure friction on mica. The observed 6-fold symmetry of the friction force was explained by commensurability of the interface (substrate and slider structure match) that led to high friction, whereas incommensurability (nonmatching) of the interface led to very low friction, i.e., superlubricity,[7] which was at least 3 times smaller than the commensurate case. Commensurability of an interface, however, is not a necessary condition for friction anisotropy. In fact, studies using atomic force microscopy (AFM)[8] to characterize friction at the single asperity level using a nanoscale probe or tip have reported significant friction anisotropy, where at least one of two sliding surfaces was noncrystalline.[9,10] Friction anisotropy has also been observed between AFM tips and surfaces with tilted molecular groups such as lipid monolayers.[5,11−13]

Many AFM-based studies of friction anisotropy have focused on two-dimensional (2D) materials, including graphene, MoS_2 and hBN. Such studies have used two different approaches to measuring friction anisotropy: manipulating crystalline structures on a 2D material with an AFM probe in different directions, or putting the AFM probe in direct contact with the 2D material and scanning in different directions (which may or may not involve rotating the sample with respect to the tip). The first approach has been applied to nanostructures (MoO_3 manipulated on MoS_2,[4] Au islands on MoS_2,[14] and carbon nanotubes on HOPG[15]) or mesas of multilayer 2D materials (graphite mesas on HOPG[16] and graphite/hBN heterojunction mesas[17]). Mesa manipulation of MoS_2 on MoS_2 was also modeled using molecular dynamics (MD) simulations.[18,19] In all these studies, the measured friction force exhibited 6-fold symmetry (i.e., the friction patterns repeat every 60°), revealing the hexagonal nature of the underlying lattice structure.

The second approach to measuring friction anisotropy on 2D materials is to slide an AFM probe directly on a substrate. During the AFM measurements, the direction in which the end of the cantilever is pulled, here referred to *"scanning direction"*, can be controlled; however, the actual path of the tip apex would slightly deviate with respect to scanning direction. In practice, probing friction in different angular scanning directions is difficult because most AFM setups are restricted to measuring lateral force only parallel to the scanning direction (i.e., perpendicular to the cantilever axis). Measuring friction anisotropy requires the ability to either rotate the sample with respect to the cantilever scanning direction (see Figure S1a) via a specially designed stage as done, e.g., in ref 20, or a method to calibrate forces and pull the AFM tip along

Received: May 25, 2020
Accepted: August 3, 2020
Published: August 3, 2020

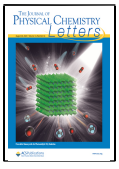

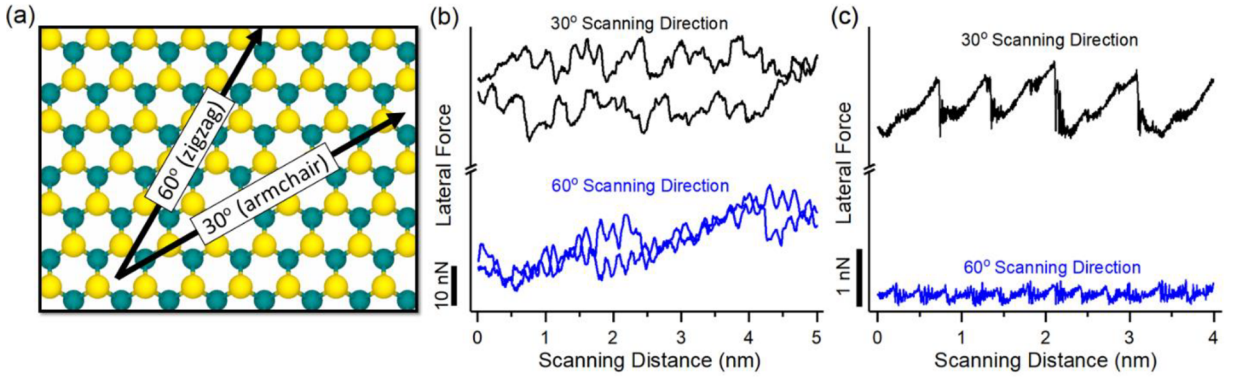

Figure 1. (a) Top view of monolayer MoS_2 in the simulations where the 30 and 60° scanning directions are identified, corresponding to the armchair and zigzag crystallographic directions of the MoS_2 lattice. (b) Representative experimental friction loops (scanning forward and backward) obtained from scanning the Si tip on bulk MoS_2 in the 30 and 60° directions. The long axis of the cantilever points along the 90° direction. (c) Representative friction traces obtained from MD simulations of dragging the model tip along the 30 and 60° directions.

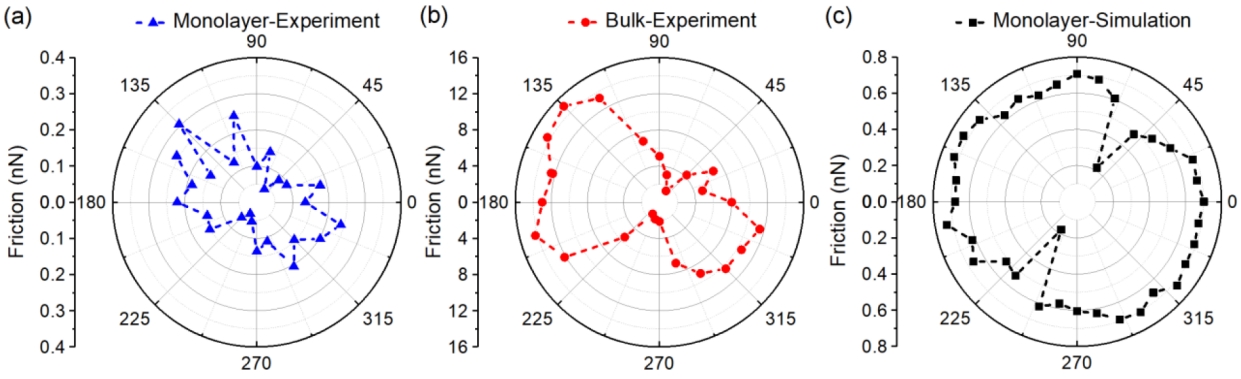

Figure 2. Friction anisotropy measured using AFM on (a) monolayer MoS_2 with a UNCD tip and (b) bulk MoS_2 with a Si/SiO_2 tip, as well as the (c) MD simulations of monolayer MoS_2 with a SiO_2 model tip. The data sets in (a) and (b) were rotated 30 and 15° clockwise, respectively, so that the experimental low friction axes approximately coincide with the low friction axis in the simulation. Dashed lines are guides for the eye only.

different scanning directions (see Figure S1b) as done, e.g., in ref 21. In cases where the sample was rotated relative to the scanning direction, some studies reported 60° periodicity (i.e., 6-fold symmetry), including measurements on monolayer graphene,[22−24] while others[25−29] observed 180° periodicity (i.e., 2-fold symmetry). The latter was attributed to out-of-plane elastic deformation of the substrate resulting from oriented linear wrinkles (sometimes referred to as ripples) in the 2D material where scanning perpendicular to the wrinkles led to higher friction. In cases where the sample was fixed and the AFM tip pulled in different directions, a 6-fold symmetry with low friction along the zigzag direction (the $\langle 11\bar{2}0 \rangle$ direction) was observed on graphite.[21,30]

To understand the origins of these very different observations and interpretations, we investigated friction anisotropy of nanoscale tips sliding on MoS_2 using complementary AFM experiments and MD simulations. MoS_2 was chosen as the sample because it is a frequently studied member of the 2D material family with a variety of applications and, more specifically, because of its potential to provide ultralow friction as a next generation solid lubricant.[31] The AFM experiments were performed on monolayer and bulk MoS_2 in ultrahigh vacuum (UHV), precluding multiple parameters that could affect friction in ambient conditions including contamination and capillary condensation. The experimental setup is illustrated schematically in Figure S2a and detailed information about the methods is available in Supporting Information section S1. Orientation-dependent friction measurements were obtained by changing the scanning direction with respect to the sample in 15° increments, with the relative surface orientation between the tip and sample remaining constant throughout. A 5×5 nm^2 area was scanned. Lattice resolution was obtained for each scan, and examples of atomic lattice-resolved stick slip are shown in Figure S3. Figure 1b shows two representative friction loops from the AFM lateral force measurements on monolayer MoS_2 corresponding to scanning in the 30° and 60° directions (see Supplementary Information section S5 for force calibration). It should be noted that, due to the rotational degree of freedom of the sample approach mechanism of the AFM used here,[32] the orientation of the scanning direction with respect to the crystallographic orientation of the MoS_2 samples could not be controlled. Therefore, in all cases, we used the lattice resolution images to identify the crystal orientation and rotate the experimental data set accordingly (by an amount indicated in each figure caption) so that the low friction directions (the zigzag directions) in both experiments and simulations are the same. The energy dissipated per scan cycle (i.e., area of the friction loop) in Figure 1b is almost 11 times higher in the 30° scanning direction compared to the 60° direction.

MD simulations enabled friction anisotropy to be characterized using both possible measurement approaches, i.e., the tip sliding in different directions on a stationary sample or the sample rotating as the tip slides in one direction. The MD

https://dx.doi.org/10.1021/acs.jpclett.0c01617
J. Phys. Chem. Lett. 2020, 11, 6900−6906

model consisted of an amorphous SiO_2 tip apex sliding over monolayer 1H-MoS_2 on a crystalline silicon substrate; see Figure S2b and details in Supporting Information section S1. Then, a lateral force microscopy experiment was mimicked by applying a 6 nN normal load to the tip and displacing the tip along the surface in different angular directions (with the scanning direction of 0°, 60°, etc. being along the zigzag direction as shown in Figure 1a). Representative friction traces from the MD simulations are shown in Figure 1c. In both experiments and simulations, friction exhibits strong anisotropy, where multiple frictional characteristics (e.g., friction trace periodicity, peak or average friction force) vary with scanning direction (additional friction traces from the simulations are shown in Figure S4). However, the major difference between the friction traces obtained by scanning in different directions is the magnitude of the friction, quantified here by the average friction force.

Figure 2 summarizes the average friction for monolayer or bulk MoS_2 measured with the scanning direction changed incrementally in steps of a few degrees (increments of 15° in experiments and 10° in simulations) without changing the relative orientation of the sample and cantilever. Note that we cannot quantitatively compare the results between simulation and experiment due to the differences in the tip material and size, and scanning velocity and load that affect the magnitude of the friction.[33] However, friction consistently exhibits 180° periodicity (i.e., 2-fold symmetry) in experiment and simulation and for both monolayer and bulk MoS_2 samples. The anisotropy ratio (ratio of the maximum to the minimum friction) was calculated to be 4.1, 5.7, and 3.6 for the experimental monolayer, the experimental bulk, and the MD monolayer MoS_2, respectively.

On the basis of the crystal symmetry of the MoS_2, a periodicity of 60° would have been expected, with low friction axes along the zigzag directions and high friction around the armchair axes.[21,22] In the MD model, the 0°, 60°, and 120° scanning axes coincide with the zigzag crystallographic direction of MoS_2 (see Figure 1a). However, low friction was obtained in simulations of scanning along only one of the zigzag directions (i.e., 60°). As briefly discussed at the beginning of this Letter, several previous studies have reported friction anisotropy with 60° symmetry on 2D materials including graphene, HOPG,[15] and MoS_2.[4,14] In most of these studies (with a few exceptions that will be discussed later), a crystalline−crystalline interface was established by (i) using the AFM tip to manipulate a crystalline nanostructure (e.g., CNT on HOPG,[15] MoO_3 on MoS_2,[4] and Au on MoS_2[14]) on a crystalline sample, (ii) using a tip or micromanipulator to shear a mesa (e.g., graphite mesa on HOPG[16] and graphite/hBN heterojunction mesa[17]) at an incommensurate plane, or (iii) transferring of sample material to the tip (e.g., graphite transfer to a W tip[30]). Only the last case is possible in our experiments and simulations. However, in the AFM experiments, there was no indication of material transfer to the tip based on observation of negligible change in adhesion measured before and after the friction tests (see Supporting Information section S6). In simulations, neither wear nor material transfer to the tip was observed. As well, commensurability between the tip and sample is unlikely. In experiments, the UNCD tips were composed of multiple, randomly oriented 2−5 nm nanoscale grains with amorphous grain boundaries, and likely an enhanced degree of amorphous material compared to the bulk,[34] which precludes the possibility of a commensurate, high symmetry interface between tip and substrate. Also, in the case of the Si tip (see Figure 2b), the native oxide layer on the tip established an amorphous−crystalline interface. This was also the case in our simulations where the tip was amorphous. Therefore, the friction anisotropy observed in our study occurred for an incommensurate sliding contact.

In previous studies[21,25−28,30] in which the AFM tip itself was used to probe friction anisotropy of 2D materials, both 6-fold[21,30] and 2-fold symmetric friction anisotropy[25−28] have been observed. In studies where the sample was rotated with a fixed scanning direction, 2-fold symmetry was observed.[24,25,27,28] The 2-fold symmetry was attributed to the existence of in-plane strain induced by topographic wrinkles formed due to the difference in thermal contraction of the substrate compared to the 2D material after deposition.[35−37] However, the above-mentioned studies did not provide AFM topographic evidence of the presence of these topographic wrinkles. Further, transmission electron microscopy (TEM),[38,39] MD,[40] and density functional theory (DFT)[41] based investigations that captured wrinkles on monolayer MoS_2 reported a typical wrinkle width to be around 10 nm.[39−42] However, our experimental friction results were extracted from AFM images with a scanning area of 5 nm × 5 nm, which is much smaller than the expected size of possible wrinkles. Unlike CVD growth on metal substrates, wrinkles are not expected for the CVD growth used in this study, where MoS_2 was deposited on Si. This was confirmed by larger area scans that showed no evidence of wrinkles (see Figure S6a). The lack of any wrinkle structure in the MD simulations was confirmed via height maps from MD simulations of monolayer MoS_2 (see Figure S6b). Lastly, intrinsic wrinkles induced by the substrate are not present in bulk MoS_2, for which we also observed 2-fold symmetry (see Figure 2b). Therefore, the 2-fold symmetry in our results is not due to the presence of structural features such as wrinkles on the sample.

A second previously suggested explanation of 2-fold symmetry observed on hBN is self-assembly of environmental adsorbates.[26] It was proposed that adsorbates from the environment assemble into a highly regular superlattice of stripes with a period 4−6 nm. However, our AFM measurements were performed under UHV conditions. The sample was annealed under a vacuum to drive off any adsorbates and then scanned without being exposed to air, minimizing the possibility of adsorbates on the sample. Further, the MD model was an ideal vacuum without adsorbate molecules. Therefore, the observed 2-fold symmetry of friction anisotropy in our monolayer and bulk MoS_2 cannot be attributed to the presence of an adsorbate superlattice on the substrate.

Another factor that can contribute to friction anisotropy is the energy landscape at the contact established between the tip and sample. In the classical Prandtl−Tomlinson (PT) model,[43,44] friction at the atomic scale depends on the height of the surface energy barrier (affected by several parameters such as surface roughness[45] and composition[46]) that the tip has to overcome to slide. Recent theoretical and experimental studies[20,47,48] suggested that the interaction potential at the contact interface affects the configuration of anisotropic frictional forces. Therefore, if the potential energy landscape exhibits anisotropy, this could directly explain the observed friction trends.

To obtain the energy landscape for monolayer MoS_2, we used quasi-static MD simulations. Briefly, a single atom (oxygen in this case) was used to probe the potential energy

https://dx.doi.org/10.1021/acs.jpclett.0c01617
J. Phys. Chem. Lett. 2020, 11, 6900−6906

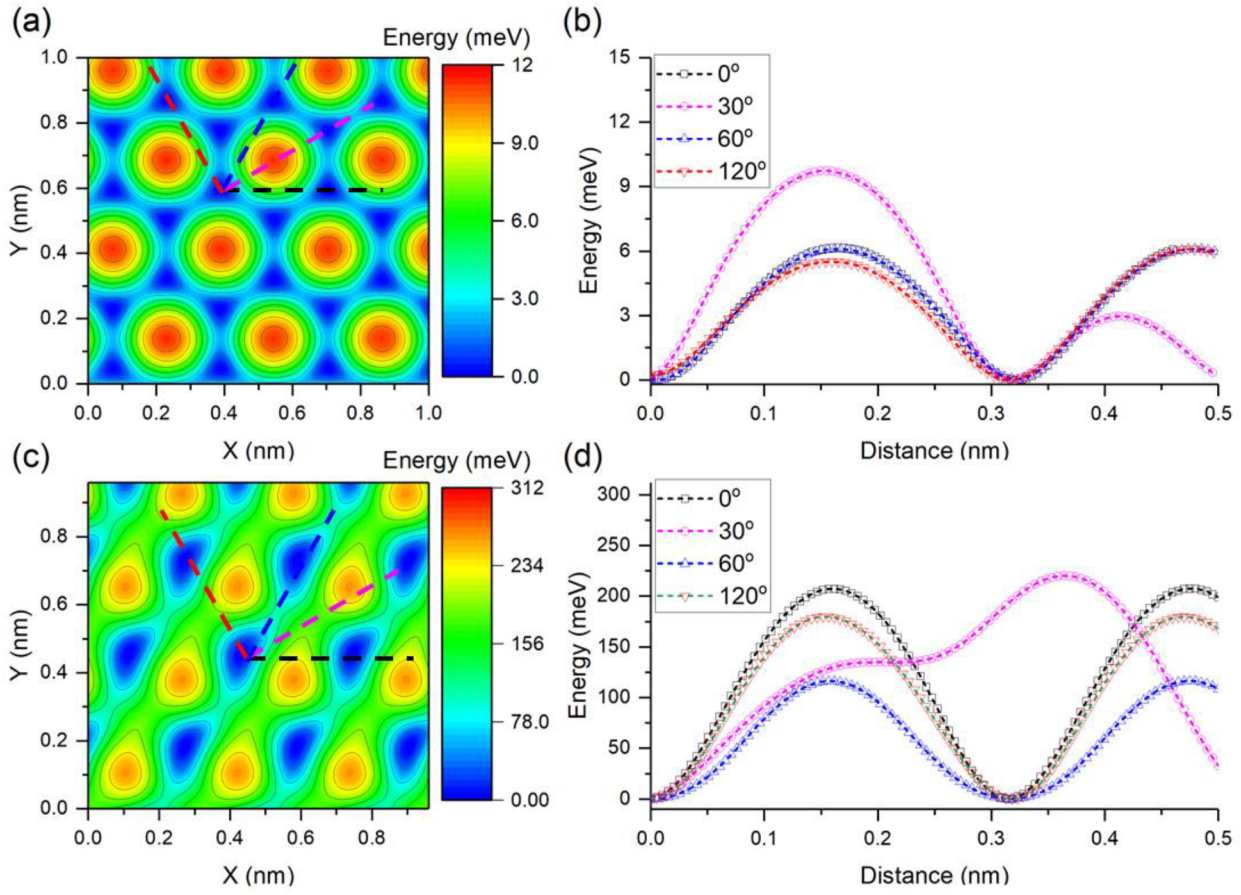

Figure 3. (a) PES obtained by raster scanning a single oxygen atom over the MoS_2 substrate. (b) Corresponding energy profiles along the zigzag directions, 0° (black dashed line), 60° (blue dashed line), 120° (red dashed line), and the armchair directions, 30° (magenta dashed line), from the PES in (a). (c) PES of the tip−sample contact. (d) Corresponding energy profiles along the 0, 30, 60, and 120° directions (black, magenta, blue, and, red dashed lines) of the tip−sample PES in (c).

of the substrate by raster scanning over the sample and calculating the minimum potential energy at each lateral position. The resultant potential energy surface (PES) is shown in Figure 3a. Probing the PES with a single atom reveals the energy landscape of the ideal MoS_2 crystalline surface. Line traces along this landscape reflect the energy barriers that an atom would have to overcome when moving along different directions relative to the crystallographic structure of the surface. As shown in Figure 3b, the energy barriers along the zigzag directions (0°, 60°, and 120°) are identical, indicating that the friction along these scanning directions should be the same, while friction along other directions would be larger since the energy barriers are higher (e.g., 30° in Figure 3b). This energy landscape therefore would lead to six "low friction axes" and 6-fold friction anisotropy.

In contrast to the single atom that is typically used to generate a PES, the tip−sample contact in an AFM experiment or MD simulation consists of tens or hundreds of atoms. Hence, the measured friction is a result of the collective behavior of an ensemble of atoms. To investigate the effect of this collective behavior, we replaced the single atom in the PES calculation with the model tip used for the friction simulations. At each lateral position of the tip, potential energy was calculated as a function of vertical position, and the minimum energy was extracted to create the PES. As shown in Figure 3c, the PES obtained from the amorphous tip apex was distinctly different from the ideal PES probed with single atom, both quantitively and qualitatively.

Representative energy barrier profiles extracted from the tip−sample PES are shown in Figure 3d. Importantly, the barrier along the 60° direction is lower than the barriers in the 0° and 120° directions, such that there is only one low friction axis, i.e., along the 60° direction. This is consistent with the 2-fold symmetric friction anisotropy observed in our experiments and simulations, suggesting that the trends can be explained directly by anisotropy of the energy landscape of the tip−surface contact. In recent years, there has been growing evidence that friction at the atomic scale depends on the quality of the contact (the degree of tip−sample interaction) in addition to the quantity of the contact (the tip−sample contact area).[49] Contact quality, which represents the strength of the total atomic interactions between the tip and sample, is a key factor affecting interfacial energy dissipation (and hence friction). For a given interface, the contact quality can change due to many factors during sliding, including relative orientation of the contacting surfaces.[30,49−52] So, the presence of any tip, regardless of its crystallinity, would distort the inherent energy landscape of the substrate, leading to observation of 2-fold symmetry. This is supported by additional simulations with a crystalline Si tip and experiments with a UNCD tip, both of which exhibit 2-fold symmetry (see Supporting Information section S9). However, further work is needed to determine the effects of different factors, such as

https://dx.doi.org/10.1021/acs.jpclett.0c01617
J. Phys. Chem. Lett. 2020, 11, 6900−6906

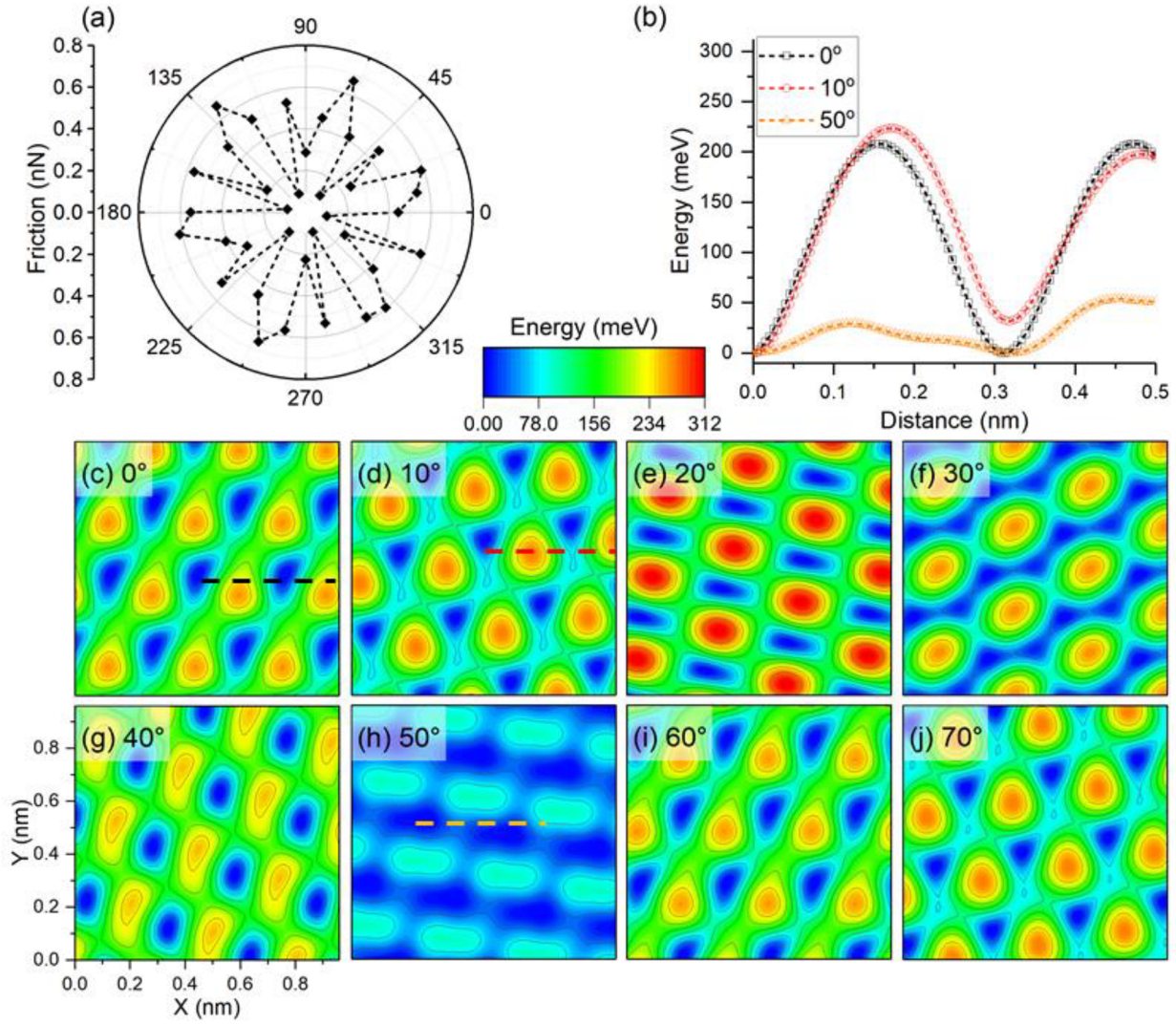

Figure 4. (a) MD simulation results for friction between the tip and MoS_2 sample as a function of sample rotational angle (setup illustrated in Figure S8), exhibiting 6-fold symmetry, where dashed lines are guides to the eye only. (b) Cross-sectional barrier profiles along scanning direction for the cases in which the sample was rotated 0° (black dashed line in (c)), 10° (red dashed line in (d)), and 50° (orange dashed line in (h)). (c)−(j) PES of the tip−sample calculated every 10° for the sample rotated counterclockwise from 0° to 70° counterclockwise.

possible sample defects, on the PES and friction anisotropy pattern. An energy landscape with some degree of symmetry-breaking distortion can be expected to arise for any tip−sample contact. The only exceptions to this would be if the tip and sample establish a highly commensurate interface, for instance by transferring some of the sample material to the tip, as mentioned explicitly in ref 30 and might have been the case in ref 21, or by having an intrinsically commensurate structure (e.g., by being oriented such that the tip and sample lattice constants match by an integer ratio). To evaluate the potential effect of sample transfer to the tip, we simulated an MoS_2 flake scanning along different angular directions on a stationary sample composed of MoS_2 monolayer and Si substrate. The simulations exhibited 6-fold friction symmetry (see Figure S7), in contrast to the 2-fold symmetry we found for any model or experimental tip.

As mentioned before, previous experimental studies measured two different kinds of friction anisotropy: anisotropy as a function of the relative rotation of the sample and tip with fixed scanning direction, or anisotropy as a function of the angle of scanning with respect to the sample with fixed relative tip/sample rotation. The simulations developed here enable both approaches to be tested with the same material system. A set of friction simulations was performed with the tip moving in the 0° scanning direction (i.e., along the *x*-direction illustrated in Figure S8) and then with the sample (MoS_2 on Si) rotated in increments of 10° while the tip orientation remained constant, as illustrated in Figure S8. The friction polar plot shown in Figure 4a exhibits 6-fold symmetry, in sharp contrast to the 2-fold symmetry observed in Figure 2c that was obtained from simulations with a fixed sample and varying the tip scanning direction.

To explain the observed friction anisotropy trend, we obtained the full-tip PES for each angular position of the sample. Figure 4b shows cross sectional energy profiles for 0°, 10°, and 50° rotations angles, and panels c−j of Figure 4 show the full PES for angles between 0° and 70°. Interestingly, the change in the relative orientation of tip and substrate caused variation of the PES at each angular position of the sample. However, the PES exhibits 60° periodicity; i.e., the 0° and 60° energy surfaces are identical, as are those at 10° and 70°, leading to 6-fold symmetric friction. In other words, when the

https://dx.doi.org/10.1021/acs.jpclett.0c01617
J. Phys. Chem. Lett. 2020, 11, 6900−6906

sample is rotated, the friction anisotropy pattern is dominated by the sample's crystallographic symmetry. This is because the configuration of the tip atoms at the interface is fixed and only the substrate (which has 60° rotational crystallographic symmetry) rotates, so there are a limited number of possible combinations for the tip−sample interface, which is governed by the sample crystallographic symmetry. So, as long as there are no other parameters affecting the anisotropy configurations, such as structural nanowrinkles,[25,26] friction measured with the sample rotated will always exhibit an anisotropy pattern in agreement with the underlying sample's crystallographic symmetry. Additional simulations of scanning in different angular directions on these rotated samples exhibited 2-fold symmetric friction, with low friction consistently observed along the two directions corresponding to the zigzag axes on each sample.

In summary, we investigated the angular dependence of atomic friction for nanoscale tips sliding on monolayer and bulk MoS_2 using AFM and MD simulations. By changing the scanning direction, we observed a 2-fold symmetry in both experiments and simulations. Comparing our results with other studies that reported friction anisotropy with 2-fold symmetry, we ruled out the possibility that the results could be explained by parallel topographical features like wrinkles. Instead, our quasi-static calculations for the tip−sample PES showed that the structure of the tip breaks the symmetry of the crystal surface, providing a distorted, low-symmetry PES that explains the observed 2-fold symmetry in friction. Thus, we identified a previously unexplored factor affecting friction anisotropy at the atomic scale, the quality of the contact formed between tip and sample, which affected the interfacial energy landscape and consequently the friction. We used MD simulations to assess the friction anisotropy produced by rotating the sample with respect to the tip, as opposed to changing the scanning direction. For this type of rotation, the friction force was anisotropic with 6-fold symmetry. This trend, consistent with the crystallographic symmetry of the underlying sample, was directly determined by the tip−sample PES. These results emphasize the important role of the tip−sample interfacial structure in determining the PES and the degree of symmetry of friction. This research provides a better fundamental understanding of the nanotribology of 2D materials, thereby opening new possibilities for the design and control of nanomechanical systems involving these materials.

■ ASSOCIATED CONTENT

Supporting Information

The Supporting Information is available free of charge at https://pubs.acs.org/doi/10.1021/acs.jpclett.0c01617.

Materials and methods for both experiments and simulations, schematics of approaches for measuring friction anisotropy, AFM experimental setup, lattice resolution images, lateral forces, polar plots, AFM topography and height map images, and MD simulation images, and tables of calibration factors, adhesion values, and LJ parameters (PDF)

■ AUTHOR INFORMATION

Corresponding Authors

Robert W. Carpick − *Department of Mechanical Engineering and Applied Mechanics, University of Pennsylvania, Philadelphia, Pennsylvania 19104, United States;* orcid.org/0000-0002-3235-3156; Email: carpick@seas.upenn.edu

Ashlie Martini − *Department of Mechanical Engineering, University of California, Merced, California 95343, United States;* orcid.org/0000-0003-2017-6081; Email: amartini@ucmerced.edu

Authors

Mohammad R. Vazirisereshk − *Department of Mechanical Engineering, University of California, Merced, California 95343, United States;* orcid.org/0000-0001-8122-7749

Kathryn Hasz − *Department of Materials Science and Engineering, University of Pennsylvania, Philadelphia, Pennsylvania 19104, United States*

Complete contact information is available at: https://pubs.acs.org/10.1021/acs.jpclett.0c01617

Author Contributions

#M.R.V. and K.H. contributed equally to this work.

Notes

The authors declare no competing financial interest.

■ ACKNOWLEDGMENTS

This work was funded by the National Science Foundation, awards CMMI-1762384 and CMMI-1761874. This work used the Extreme Science and Engineering Discovery Environment (XSEDE), which is supported by National Science Foundation Grant ACI-1548562.

■ REFERENCES

(1) Yu, S.; Zhu, H.; Eshun, K.; Shi, C.; Zeng, M.; Li, Q. Strain-Engineering the Anisotropic Electrical Conductance in ReS_2 Monolayer. *Appl. Phys. Lett.* **2016**, *108*, 191901.

(2) Xu, K.; Pan, Y.; Ye, S.; Lei, L.; Hussain, S.; Wang, Q.; Yang, Z.; Liu, X.; Ji, W.; Xu, R.; Cheng, Z. Shear Anisotropy-Driven Crystallographic Orientation Imaging in Flexible Hexagonal Two-Dimensional Atomic Crystals. *Appl. Phys. Lett.* **2019**, *115*, 063101.

(3) Manju, M. S.; Ajith, K. M.; Valsakumar, M. C. Strain Induced Anisotropic Mechanical and Electronic Properties of 2D-SiC. *Mech. Mater.* **2018**, *120*, 43−52.

(4) Sheehan, P. E.; Lieber, C. M. Nanotribology and Nanofabrication of MoO_3 Structures by Atomic Force Microscopy. *Science* **1996**, *272*, 1158−1161.

(5) Carpick, R. W.; Sasaki, D. Y.; Burns, A. R. Large Friction Anisotropy of a Polydiacetylene Monolayer. *Tribol. Lett.* **1999**, *7*, 79−85.

(6) Hirano, M.; Shinjo, K.; Kaneko, R.; Murata, Y. Anisotropy of Frictional Forces in Muscovite Mica. *Phys. Rev. Lett.* **1991**, *67*, 2642−2645.

(7) Baykara, M. Z.; Vazirisereshk, M. R.; Martini, A. Emerging Superlubricity: A Review of the State of the Art and Perspectives on Future Research. *Appl. Phys. Rev.* **2018**, *5*, 041102.

(8) Binnig, G.; Quate, C. F.; Gerber, C. Atomic Force Microscope. *Phys. Rev. Lett.* **1986**, *56*, 930−933.

(9) Kwak, M.; Shindo, H. Frictional Force Microscopic Detection of Frictional Asymmetry and Anisotropy at $(10\bar{1}4)$ Surface of Calcite. *Phys. Chem. Chem. Phys.* **2004**, *6*, 129−133.

(10) Park, J. Y.; Ogletree, D. F.; Salmeron, M.; Ribeiro, R. A.; Canfield, P. C.; Jenks, C. J.; Thiel, P. A. High Frictional Anisotropy of Periodic and Aperiodic Directions on a Quasicrystal Surface. *Science* **2005**, *309*, 1354−1356.

(11) Liley, M.; Gourdon, D.; Stamou, D.; Meseth, U.; Fischer, T. M.; Lautz, C.; Stahlberg, H.; Vogel, H.; Burnham, N. A.; Duschl, C. Friction Anisotropy and Asymmetry of a Compliant Monolayer Induced by a Small Molecular Tilt. *Science* **1998**, *280*, 273−275.

(12) Zhang, L.; Leng, Y.; Jiang, S. Tip-Based Hybrid Simulation Study of Frictional Properties of Self-Assembled Monolayers: Effects of Chain Length, Terminal Group, Scan Direction, and Scan Velocity. *Langmuir* **2003**, *19*, 9742−9747.
(13) Overney, R. M.; Takano, H.; Fujihira, M.; Paulus, W.; Ringsdorf, H. Ansiotropy in Friction and Molecular Stick-Slip Motion. *Phys. Rev. Lett.* **1994**, *72*, 3546−3549.
(14) Trillitzsch, F.; Guerra, R.; Janas, A.; Manini, N.; Krok, F.; Gnecco, E. Directional and Angular Locking in the Driven Motion of Au Islands on MoS_2. *Phys. Rev. B: Condens. Matter Mater. Phys.* **2018**, *98*, 165417.
(15) Falvo, M. R.; Steele, J.; Taylor, R. M.; Superfine, R. Gearlike Rolling Motion Mediated by Commensurate Contact: Carbon Nanotubes on HOPG. *Phys. Rev. B: Condens. Matter Mater. Phys.* **2000**, *62*, R10665.
(16) Liu, Z.; Yang, J.; Grey, F.; Liu, J. Z.; Liu, Y.; Wang, Y.; Yang, Y.; Cheng, Y.; Zheng, Q. Observation of Microscale Superlubricity in Graphite. *Phys. Rev. Lett.* **2012**, *108*, 205503.
(17) Song, Y.; Mandelli, D.; Hod, O.; Urbakh, M.; Ma, M.; Zheng, Q. Robust Microscale Superlubricity in Graphite/Hexagonal Boron Nitride Layered Heterojunctions. *Nat. Mater.* **2018**, *17*, 894−899.
(18) Onodera, T.; Morita, Y.; Nagumo, R.; Miura, R.; Suzuki, A.; Tsuboi, H.; Hatakeyama, N.; Endou, A.; Takaba, H.; Dassenoy, F.; Minfray, C.; Joly-Pottuz, L.; Kubo, M.; Martin, J. M.; Miyamoto, A. A Computational Chemistry Study on Friction of H-MoS_2. Part II. Friction Anisotropy. *J. Phys. Chem. B* **2010**, *114*, 15832−15838.
(19) Claerbout, V. E. P.; Polcar, T.; Nicolini, P. Superlubricity Achieved for Commensurate Sliding: MoS_2 Frictional Anisotropy in Silico. *Comput. Mater. Sci.* **2019**, *163*, 17−23.
(20) Fessler, G.; Sadeghi, A.; Glatzel, T.; Goedecker, S.; Meyer, E. Atomic Friction: Anisotropy and Asymmetry Effects. *Tribol. Lett.* **2019**, *67*, 59.
(21) Balakrishna, S. G.; De Wijn, A. S.; Bennewitz, R. Preferential Sliding Directions on Graphite. *Phys. Rev. B: Condens. Matter Mater. Phys.* **2014**, *89*, 245440.
(22) Almeida, C. M.; Prioli, R.; Fragneaud, B.; Cançado, L. G.; Paupitz, R.; Galvão, D. S.; De Cicco, M.; Menezes, M. G.; Achete, C. A.; Capaz, R. B. Giant and Tunable Anisotropy of Nanoscale Friction in Graphene. *Sci. Rep.* **2016**, *6*, 31569.
(23) Liu, Z.; Ma, T.; Liu, L. Optical-Assistant Characterization of Friction Anisotropy Properties of Single-Crystal Graphene Domains. *Tribol. Int.* **2017**, *110*, 131−139.
(24) Long, F.; Yasaei, P.; Yao, W.; Salehi-Khojin, A.; Shahbazian-Yassar, R. Anisotropic Friction of Wrinkled Graphene Grown by Chemical Vapor Deposition. *ACS Appl. Mater. Interfaces* **2017**, *9*, 20922−20927.
(25) Choi, J. S.; Kim, J. S.; Byun, I. S.; Lee, D. H.; Lee, M. J.; Park, B. H.; Lee, C.; Yoon, D.; Cheong, H.; Lee, K. H.; Son, Y. W.; Park, J. Y.; Salmeron, M. Friction Anisotropy-Driven Domain Imaging on Exfoliated Monolayer Graphene. *Science* **2011**, *333*, 607−610.
(26) Gallagher, P.; Lee, M.; Amet, F.; Maksymovych, P.; Wang, J.; Wang, S.; Lu, X.; Zhang, G.; Watanabe, K.; Taniguchi, T.; Goldhaber-Gordon, D. Switchable Friction Enabled by Nanoscale Self-Assembly on Graphene. *Nat. Commun.* **2016**, *7*, 10745.
(27) Lee, J. S. J. H.; Lee, S.; Jeon, J. H.; Oh, D. Y.; Shin, M.; Lee, M. J.; Shinde, S.; Ahn, J. H.; Roh, C. J.; Lee, J. S. J. H.; Park, B. H. Universality of Strain-Induced Anisotropic Friction Domains on 2D Materials. *NPG Asia Mater.* **2018**, *10*, 1069−1075.
(28) Cao, X.; Gan, X.; Lang, H.; Yu, K.; Ding, S.; Peng, Y.; Yi, W. Anisotropic Nanofriction on MoS_2 with Different Thicknesses. *Tribol. Int.* **2019**, *134*, 308−316.
(29) Choi, J. S.; Kim, J.-S.; Byun, I.-S.; Lee, D. H.; Hwang, I. R.; Park, B. H.; Choi, T.; Park, J. Y.; Salmeron, M. Facile Characterization of Ripple Domains on Exfoliated Graphene. *Rev. Sci. Instrum.* **2012**, *83*, 073905.
(30) Dienwiebel, M.; Verhoeven, G. S.; Pradeep, N.; Frenken, J. W. M.; Heimberg, J. A.; Zandbergen, H. W. Superlubricity of Graphite. *Phys. Rev. Lett.* **2004**, *92*, 126101.
(31) Vazirisereshk, M. R.; Martini, A.; Strubbe, D. A.; Baykara, M. Z. Solid Lubrication with MoS_2: A Review. *Lubricants* **2019**, *7*, 57.
(32) Dai, Q.; Vollmer, R.; Carpick, R. W.; Ogletree, D. F.; Salmeron, M. A Variable Temperature Ultrahigh Vacuum Atomic Force Microscope. *Rev. Sci. Instrum.* **1995**, *66*, 5266−5271.
(33) Dong, Y.; Li, Q.; Martini, A. Molecular Dynamics Simulation of Atomic Friction: A Review and Guide. *J. Vac. Sci. Technol., A* **2013**, *31*, 030801.
(34) Sumant, A. V.; Grierson, D. S.; Gerbi, J. E.; Birrell, J.; Lanke, U. D.; Auciello, O.; Carlisle, J. A.; Carpick, R. W. Toward the Ultimate Tribological Interface: Surface Chemistry and Nanotribology of Ultrananocrystalline Diamond. *Adv. Mater.* **2005**, *17*, 1039−1045.
(35) Egberts, P.; Han, G. H.; Liu, X. Z.; Johnson, A. T. C.; Carpick, R. W. Frictional Behavior of Atomically Thin Sheets: Hexagonal-Shaped Graphene Islands Grown on Copper by Chemical Vapor Deposition. *ACS Nano* **2014**, *8*, 5010−5021.
(36) Obraztsov, A. N.; Obraztsova, E. A.; Tyurnina, A. V.; Zolotukhin, A. A. Chemical Vapor Deposition of Thin Graphite Films of Nanometer Thickness. *Carbon* **2007**, *45*, 2017−2021.
(37) Hattab, H.; N'Diaye, A. T.; Wall, D.; Klein, C.; Jnawali, G.; Coraux, J.; Busse, C.; Van Gastel, R.; Poelsema, B.; Michely, T.; Meyer Zu Heringdorf, F. J.; Horn-Von Hoegen, M. Interplay of Wrinkles, Strain, and Lattice Parameter in Graphene on Iridium. *Nano Lett.* **2012**, *12*, 678−682.
(38) Wang, W. L.; Bhandari, S.; Yi, W.; Bell, D. C.; Westervelt, R.; Kaxiras, E. Direct Imaging of Atomic-Scale Ripples in Few-Layer Graphene. *Nano Lett.* **2012**, *12*, 2278−2282.
(39) Brivio, J.; Alexander, D. T. L.; Kis, A. Ripples and Layers in Ultrathin MoS_2 Membranes. *Nano Lett.* **2011**, *11*, 5148−5153.
(40) Wang, J.; Namburu, R. R.; Dubey, M.; Dongare, A. M. Origins of Ripples in CVD-Grown Few-Layered MoS_2 Structures under Applied Strain at Atomic Scales. *Sci. Rep.* **2017**, *7*, 40862.
(41) Miró, P.; Ghorbani-Asl, M.; Heine, T. Spontaneous Ripple Formation in MoS_2 Monolayers: Electronic Structure and Transport Effects. *Adv. Mater.* **2013**, *25*, 5473−5475.
(42) Zheng, Y.; Chen, J.; Ng, M. F.; Xu, H.; Liu, Y. P.; Li, A.; O'Shea, S. J.; Dumitrică, T.; Loh, K. P. Quantum Mechanical Rippling of a MoS_2 Monolayer Controlled by Interlayer Bilayer Coupling. *Phys. Rev. Lett.* **2015**, *114*, 065501.
(43) Prandtl, L. Ein Gedankenmodell Zur Kinetischen Theorie Der Festen Körper. *Z. Angew. Math. Mech.* **1928**, *8*, 85−106.
(44) Tomlinson, G. A. A. CVI. A Molecular Theory of Friction. *Philos. Mag.* **1929**, *7*, 905−939.
(45) Ye, Z. J.; Otero-De-La-Roza, A.; Johnson, E. R.; Martini, A.; Ye, Zhijiang; Otero-de-la-Roza, Alberto; Erin, R. J.; A. M. Oscillatory Motion in Layered Materials: Graphene, Boron Nitride, and Molybdenum Disulfide. *Nanotechnology* **2015**, *26*, 165701.
(46) Cammarata, A.; Polcar, T. Overcoming Nanoscale Friction Barriers in Transition Metal Dichalcogenides. *Phys. Rev. B: Condens. Matter Mater. Phys.* **2017**, *96*, 085406.
(47) Takoutsing, C. S.; Djuidjé Kenmoé, G.; Kofané, T. C. Effects of Anisotropy and Substrate Shape on Atomic Friction Force in Two-Dimensional Model. *Tribol. Lett.* **2017**, *65*, 107.
(48) Perez-Rodriguez, A.; Barrena, E.; Fernández, A.; Gnecco, E.; Ocal, C. A Molecular-Scale Portrait of Domain Imaging in Organic Surfaces. *Nanoscale* **2017**, *9*, 5589−5596.
(49) Li, S.; Li, Q.; Carpick, R. W.; Gumbsch, P.; Liu, X. Z.; Ding, X.; Sun, J.; Li, J. The Evolving Quality of Frictional Contact with Graphene. *Nature* **2016**, *539*, 541.
(50) de Wijn, A. S. Flexible Graphene Strengthens Friction. *Nature* **2016**, *539*, 502−503.
(51) Kim, W. K.; Falk, M. L. Atomic-Scale Simulations on the Sliding of Incommensurate Surfaces: The Breakdown of Superlubricity. *Phys. Rev. B: Condens. Matter Mater. Phys.* **2009**, *80*, 235428.
(52) Li, Q.; Tullis, T. E.; Goldsby, D.; Carpick, R. W. Frictional Ageing from Interfacial Bonding and the Origins of Rate and State Friction. *Nature* **2011**, *480*, 233−236.

https://dx.doi.org/10.1021/acs.jpclett.0c01617
J. Phys. Chem. Lett. 2020, 11, 6900−6906